
Article:
Eskandari, Mahdi, Burr, Alister Graham orcid.org/0000-0001-6435-3962, Cumanan, Kanapathippillai orcid.org/0000-0002-9735-7019 et al. (1 more author) (2024) CGAN-Based Slow Fluid Antenna Multiple Access. IEEE wireless communications letters. ISSN 2162-2337

https://doi.org/10.1109/LWC.2024.3452941

This article has been accepted for publication in IEEE Wireless Communications Letters. This is the author's version which has not been fully edited and content may change prior to final publication. Citation information: DOI 10.1109/LWC.2024.3452941

cGAN-based Slow Fluid Antenna Multiple Access

Mahdi Eskandari, *Member, IEEE*, Alister Graham Burr, *Senior Member, IEEE*, Kanapathippillai Cumanan, *Senior Member, IEEE*, and Kai-Kit Wong, *Fellow, IEEE*

***Abstract*—The emerging fluid antenna system (FAS) technology enables multiple access utilizing deep fades in the spatial domain. This paradigm is known as fluid antenna multiple access (FAMA). Despite conceptual simplicity, the challenge of finding the position (a.k.a. port) that maximizes the signal-to-interference plus noise ratio (SINR) at the FAS receiver output, cannot be overstated. This letter proposes to take only a few SINR observations in the FAS space and infer the SINRs for the missing ports by employing a conditional generative adversarial network (cGAN). With this approach, port selection for FAMA can be performed based on a few SINR observations. Our simulation results illustrate great reductions in the outage probability (OP) with only few observed ports, showcasing the efficacy of our proposed scheme.**

***Index Terms*—Antenna position selection, fluid antenna systems, machine learning, conditional generative adversarial networks, outage, fluid antenna multiple access.**

I. Introduction

MULTIPLE-input multiple-output (MIMO) systems have been a key technology in the physical layer of wireless communications. The current fifth-generation (5G) is relying on the use of 64 antennas at the base station (BS) to meet the capacity requirement [1]. Although antenna sizes tend to decrease with higher frequency bands, replicating this trend at the user equipment (UE) is unlikely due to space constraints. To achieve more spatial diversity at the UE, the emerging fluid antenna system (FAS) technology is appealing [2], [3].

FAS represents shape-flexible position-flexible antenna systems and was first introduced by Wong *et al.* in [4], [5]. Since then, there have been many studies reporting the fundamental performance of FAS under different channel models [6], [7], [8], [9], [10]. The MIMO-FAS setup in which multiple fluid[1] antennas are utilized at both the transmitter and receiver ends was also considered in [11]. A more complete list of recent work on FAS can be found in [12]. Experimental results on FAS have also recently been reported in [13], [14].

Multiple access in the spatial domain can also be achieved in a very different way using FAS. In [15], [16], the concept of fluid antenna multiple access (FAMA) was introduced. In particular, if the FAS switches its antenna position to the port where the sum-interference signal cancels on a per-symbol basis, then 100+ UEs can be accommodated on the same channel. Nonetheless, switching the antenna position on a symbol-by-symbol basis not only is practically challenging but identifying the best port in this time scale is also not known to be possible. For this reason, [17] proposed a much simpler version, referred to as *slow* FAMA, which only switches the position once during each channel coherence time to maximize the average signal-to-interference plus noise ratio (SINR).

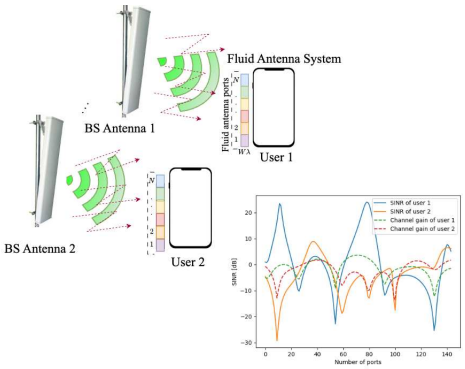

Fig. 1: Illustration of the slow FAMA concept.

Even though slow FAMA is practically attractive, it requires SINR measurements at all the possible positions of the FAS. Note that FAS has fine spatial resolution and hence the number of switchable positions is large. To deal with this issue, [18] estimated the channel gains of only a limited number of FAS ports and then used a long-short-term memory (LSTM)-based approach to infer the channel gains of the remaining ports. In [19], another learning-based scheme was presented to solve the port selection problem in a FAS in time-varying environments. The slow FAMA problem was also addressed using a LSTM approach in [20]. These approaches are possible as the FAS ports are close to each other with correlation to exploit.

Furthering the aforementioned efforts, the conditional generative adversarial network (cGAN) holds a great promise due to its ability to learn from both observed data and conditional information [21]. As a result of the intricate relationships and correlations among the FAS ports, cGANs are expected to be effective at estimating the SINRs for closely spaced FAS ports conditioned on the observation of some ports. Presumably, by conditioning the generation process on the available port-SINR observations, a trained cGAN can learn the underlying patterns and dependencies within the data, empowering it to generate plausible SINR estimates for the remaining ports.

In this letter, we develop an efficient port selection approach for slow FAMA employing cGANs to generate the missing SINR points with least port observations. The cGAN-based solution generates the envelope of port-SINR using the available SINR points as labels. Remarkably, the results reveal its efficacy by accurately generating the missing SINRs even when fewer than 20% of the SINR points are observed.

II. System Model

A. System Model

As shown in Fig. 1, a downlink multiuser system is considered where a BS equipped with U fixed-position antennas is

M. Eskandari, A. G. Burr and K. Cumanan are with the School of Physics, Engineering and Technology, University of York, YO10 5DD, U.K. (e-mail: {mahdi.eskandari, alister.burr, kanapathippillai.cumanan}@york.ac.uk).

K. Wong is with the Department of Electronic and Electrical Engineering, University College London, WC1E 7JE, U.K. He is also affiliated with Yonsei Frontier Lab, Yonsei University, Korea (e-mail: kitwong@ieee.org).

[1]Note that the word 'fluid' here does not imply the use of actual fluidic materials for antennas but stresses the flexible nature of the antennas.

communicating with U UEs. An N-port FAS is deployed at each UE, allowing the radiating element to be switched to the most effective port for optimizing system performance. Each user's FAS has ports distributed over a linear scale of size $W\lambda$, where λ is the carrier wavelength.[2] It is assumed that the u-th BS antenna is assigned to transmit information signals to UE u. Furthermore, ignoring the delay caused by port switching,[3] the received signal at port k of UE u is given by

$$y_k^{(u)} = g_k^{(u,u)} x_u + \sum_{\substack{u'=1 \\ u' \neq u}}^{U} g_k^{(u',u)} x_{u'} + n_k^{(u)}, \tag{1}$$

where $g_k^{(u',u)}$ is the complex channel coefficient from antenna u' of the BS to port k of UE u with zero mean and variance of σ^2, x_u denotes the transmitted symbol dedicated to UE u and n_k is the complex Gaussian noise at port k of UE u with zero mean and variance of σ_n^2. Based on (1), the port selection problem to maximize the SINR at UE u is given by [17]

$$k_u^{\text{s-FAMA}} = \arg\max_k \gamma_k, \tag{2}$$

where we have the SINR at port k as

$$\gamma_k = \frac{|g_k^{(u,u)}|^2}{\sum_{\substack{u'=1 \\ u' \neq u}}^{U} |g_k^{(u',u)}|^2 + \sigma_n^2}. \tag{3}$$

The outage probability (OP), defined based on a target SINR threshold, γ, is expressed as

$$p_{\text{out}} = \Pr\left\{ \max_k \gamma_k \leq \gamma \right\}. \tag{4}$$

Also, the system multiplexing gain can be defined as [17]

$$m = U(1 - p_{\text{out}}), \tag{5}$$

which estimates the capacity scaling of the network.

B. Channel Model

Given that the channel follows a complex Gaussian distribution with zero mean and variance of σ^2, the magnitude follows a Rayleigh distribution with probability distribution function

$$p_{\left|g_k^{(u,u)}\right|}(r) = \frac{2r}{\sigma^2} e^{\frac{-r^2}{\sigma^2}}, \text{ for } r \geq 0, \tag{6}$$

with $\mathbb{E}\{|g_k^{(u,u)}|^2\} = \sigma^2$. Since the FAS ports can be very close to each other, their channels are correlated. For a line-shaped fluid antenna of length $W\lambda$ in rich isotropic scattering environments, the cross-correlation of the channels between any two ports follows the Jake's model [22] so that

$$\mathbb{E}\left\{ g_k^{(u,u)} g_\ell^{(u,u)*} \right\} \triangleq \phi_{k,\ell} = \frac{\sigma^2}{2} J_0\left(\frac{2\pi(k-\ell)W}{N-1} \right), \tag{7}$$

where $J_0(.)$ is the zero-order Bessel function of the first kind. This model follows from the one used in [20] such that the channels for all the ports can be expressed as

$$\underbrace{\begin{bmatrix} g_1 \\ g_2 \\ \vdots \\ g_N \end{bmatrix}}_{\mathbf{g}} = \underbrace{\begin{bmatrix} a_{11} & a_{12} & \dots & a_{1N} \\ a_{21} & a_{22} & \dots & a_{2N} \\ \vdots & & \ddots & \\ a_{N1} & a_{N2} & \dots & a_{NN} \end{bmatrix}}_{\mathbf{A}} \underbrace{\begin{bmatrix} w_1 \\ w_2 \\ \vdots \\ w_N \end{bmatrix}}_{\mathbf{w}}, \tag{8}$$

where $\mathbf{w} \in \mathbb{C}^{N\times 1}$ represents a vector, each element of which follows an independent and identically distributed (i.i.d.) zero-mean complex Gaussian random variable with unit variance. Here, the superscript (u,u) is omitted to simplify the notations. Additionally, $\mathbf{A} \in \mathbb{C}^{N\times N}$ denotes a matrix designed to establish correlations between the ports of the FAS. To design $\mathbf{A}$, initially based on (7), stacking all the values of $\phi_{k,\ell}$ for $k, p = 1, 2, \dots, N, k \neq \ell$, will result in the $N \times N$ matrix $\mathbf{\Phi}$. Then using eigenvalue decomposition, $\mathbf{\Phi}$ can be written as $\mathbf{\Phi} = \mathbf{U}\mathbf{\Sigma}\mathbf{U}^T$. Thus, by $\mathbf{A} = \mathbf{U}\mathbf{\Sigma}^{1/2}$, (7) will be met [20].[4]

C. Port Selection

For slow FAMA. the objective is to enhance system performance by dynamically selecting the optimal port that maximizes the received SINR at each UE. As long as the receiver has access to the SINR across all of the ports, selecting the optimal port would be straightforward. However, in the FAS architecture, many ports are often located close together, so it is impossible to access all SINR ports at once. Consequently, estimating the channel gain of each individual port becomes infeasible. Nonetheless, assuming that only a subset $\mathcal{K}$ of ports are observed and the remaining $\mathcal{P}$ ports are unobserved but inferred, the port selection problem in (2) becomes[5]

$$k_u^{\text{s-FAMA}} = \arg\max \left\{ \{\gamma_k\}_{k\in\mathcal{K}}, \{\tilde{\gamma}_p\}_{p\in\mathcal{P}} \right\}, \tag{9}$$

where $\tilde{\gamma}_p$ denotes the unobserved SINR at port p.

Based on the optimization problem (9), it becomes apparent that estimating the SINR of the unobserved ports could significantly reduce the complexity of the port selection problem, especially when compared to the scenarios where all ports are observed. By doing so, the computational burden associated with exhaustive SINR observation diminishes, rendering the task more manageable and resource-efficient.

III. cGAN-based Algorithm

A standard generative adversarial network (GAN) comprises a generative model (a.k.a. generator), and an adversarial model (a.k.a. discriminator), engaged in competitive interaction. The generator is tasked for synthesising data samples, while the discriminator aims to distinguish between real and synthetic samples. Through iterative training, GANs learn to generate increasingly realistic outputs, capturing complex data distributions across diverse domains. On the other hand, cGANs

[2]The model can be easily extended to cope with a two-dimensional FAS at each UE. In this letter, however, we consider a linear FAS for simplicity.

[3]This is reasonable for reconfigurable pixel-based FASs in [14].

[4]Large-scale fading is not considered in our model because the effects of large-scale fading and distance-dependent path loss are normally cancelled using power control to normalize the performance over different users.

[5]In this letter, an 'observed' port means that the port's SINR is available.

This article has been accepted for publication in IEEE Wireless Communications Letters. This is the author's version which has not been fully edited and content may change prior to final publication. Citation information: DOI 10.1109/LWC.2024.3452941

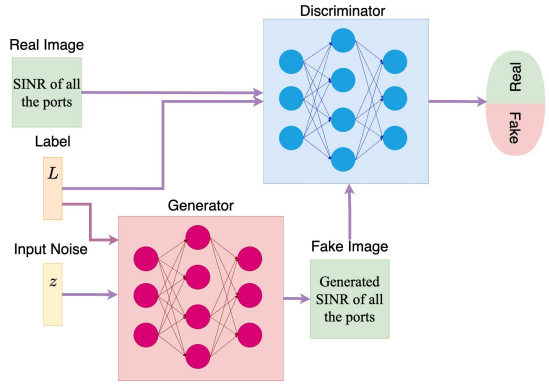

Fig. 2: A sample architecture of a cGAN.

introduce an extension by incorporating additional conditioning information into the generative process. Unlike standard GANs that generate data samples solely from random noise vectors as the input of the generator network, cGANs take into account auxiliary input, in the form of labels or context information, to generate outputs conditioned on specific attributes or characteristics, as illustrated in Fig. 2. The integration of conditioning information empowers cGANs to generate highly customizable and controllable outputs. cGANs possess unique ability to generate realistic data samples based on a given set of observations. In the context of channel gain estimation for unobserved ports, this characteristics proves indispensable. By leveraging the available observations, a cGAN algorithm can intelligently infer the channel gains of the remaining ports. Thus, the proposed cGAN algorithm not only offers a means to mitigate the complexity of port selection but also capitalizes on the inherent correlations among ports to provide accurate estimations of channel gains, thereby enhancing the overall efficiency and effectiveness of the communication system.

A. Data Generation

To employ cGAN, the first step is to generate a dataset and the corresponding labels. To do so, first the SINR vector $\boldsymbol{\gamma} \in \mathbb{R}^N$ is generated using (3), where the n-th element of $\boldsymbol{\gamma}$ is γ_n. Then it will be reshaped to a matrix of size $\sqrt{N} \times \sqrt{N}$ denoted by $\boldsymbol{\Gamma}$.[6] The labels $\mathbf{L}$ for training are included in the vector of length $|\mathcal{K}|$ storing the SINRs of the observed ports. To normalize the dataset for training while preserving its distribution, we employ a max-min normalization technique. This involves transforming each data point such that its value falls within the range of $[0, 1]$. The process works by subtracting the minimum value of the dataset from each data point and then dividing by the difference between the maximum and minimum values. This ensures that the transformed data maintains the relative relationships between its values, preserving the dataset's overall distribution. Finally, after generating a sufficient number of data samples, the dataset is saved as the tuple $\mathbb{D} = \{\boldsymbol{\Gamma}, \mathbf{L}\}$.

[6]We assume that N is a perfect square number. However, if N is not a perfect square, we can pad $\boldsymbol{\Gamma}$ with zeros to create a square matrix. This step is necessary because during the training process, the cGAN will perform convolutions on the input, which necessitates a square matrix.

B. Objective of cGAN

In a typical cGAN architecture, there are two networks, a generative model G parameterized by the neural network (NN) weights θ and a discriminative model D parameterized by the NN weights ψ. To learn a generator distribution p_g over the dataset $\mathbb{D}$, the generator builds a mapping function from a prior normal noise distribution $p_Z(z)$ and the labels from the dataset to the data space as $G(z;\theta)$. On the other hand, the discriminator outputs a scalar value to distinguish whether the input sample and the corresponding label are real or generated by the generator network. Both generator G and discriminator D are trained simultaneously. The NN weights of the generator are adjusted to minimize $\log(1-D(G(\mathbf{z}|\mathbf{L})))$, which represents the generator loss, assessing the generator's ability to produce data that is indistinguishable from real data by the discriminator. Furthermore, the NN weights of the discriminator are modified to minimize $\log(D(\mathbf{G}|\mathbf{L}))$, which corresponds to the discriminator loss, quantifying the discriminator's effectiveness in distinguishing between real and generated samples. Moreover, to ensure the right direction of the generator optimization, we add an $\mathcal{L}_2$ loss [24], [25] to the cGAN loss, which is expressed as

$$\mathcal{L}_2 = \mathbb{E}\{\|G(\mathbf{z}|\mathbf{L}) - \boldsymbol{\Gamma}\|^2\}. \tag{10}$$

This $\mathcal{L}_2$ loss function measures the discrepancy between the generated output and the true data, thus encouraging the generator to produce more accurate and realistic results. Hence, the overall cGAN network can be viewed as a two-player min-max game with the value function $V(G, D)$ [21]

$$\begin{aligned}\min_G \max_D V(G,D) = {} & \mathbb{E}_{\mathbf{x}\sim p_{\boldsymbol{\Gamma}}(x)}\{\log(D(\mathbf{x}|\mathbf{L}))\} \\ & + \mathbb{E}_{\mathbf{z}\sim p_Z(\mathbf{z})}\{\log(1 - D(G(\mathbf{z}|\mathbf{L})))\} \\ & + t\mathcal{L}_2,\end{aligned} \tag{11}$$

where t is a weighting factor emphasizing the importance of the $\mathcal{L}_2$ norm. The detailed parameters of the cGAN networks are provided in Table I. The inference complexity is primarily determined by the generator's forward pass, given by

$$O\left(\sum_{i=1}^{L} n_i \times m_i\right), \tag{12}$$

where L is the number of layers, n_i represents the number of neurons in layer i and m_i denotes the number of connections from layer $i-1$ to layer i.

IV. Simulation Results

In this section, we provide the simulation results to evaluate the efficacy of the proposed algorithm. The simulations were conducted using Python 3.10.0, with Keras employed for the development of the cGAN.[7] Rayleigh fading was considered across all the simulations involving channel envelopes, with a linear structure adopted for the fluid antenna configuration. The number of ports was set to $N = 144$ and the dataset was generated using (3). We generated 4×10^5 data samples to train

[7]The source code of the Keras implementation of the cGAN is accessible via https://keras.io/examples/generative/conditional_gan/.

This article has been accepted for publication in IEEE Wireless Communications Letters. This is the author's version which has not been fully edited and content may change prior to final publication. Citation information: DOI 10.1109/LWC.2024.3452941

TABLE I: cGAN-based port selection structures.

Discriminator	
Layer Type	**Output Shape, Stride / Padding**
InputLayer	(12, 12, X)
Conv2D	(6, 6, 64), 2 / Same
LeakyReLU	(6, 6, 64)
Conv2D	(3, 3, 128), 2 / Same
LeakyReLU	(3, 3, 128)
GlobalMaxPooling2D	(128,)
Dense	(1,)

Generator	
Layer Type	**Output Shape, Stride / Padding**
InputLayer	($\|\mathbf{Y}\|$,)
Dense	(27,)
LeakyReLU	(27,)
Reshape	(3, 3, $\|\mathbf{Y}\|$)
Conv2DTranspose	(6, 6, 128), 2 / Same
LeakyReLU	(6, 6, 128)
Conv2DTranspose	(12, 12, 128), 2 / Same
LeakyReLU	(12, 12, 128)
Conv2D	(12, 12, 1)

the cGAN. The number of observed ports is sampled evenly across the ports. The batch size is set to be 32 and the learning rate for the generator and discriminator is set to be 0.0003 and 0.0002, respectively. Moreover, the weighting factor t for the $\mathcal{L}_2$ loss is set to be 40. Also, the number of epochs for training the cGAN is 1000. Furthermore, the input noise for the generator $\mathbf{z}$ is sampled from the Gaussian distribution with zero mean and unit variance with the dimension of 128. Thus, the input $\mathbf{Y}$ of the generator is $\mathbf{Y} = \mathbf{z} + \mathbf{L}$. Also. the input channel X for the discriminator consists of the number of labels, i.e., $|\mathcal{K}|$. That is $X = |\mathcal{K}|$. Furthermore, the average signal-to-noise ratio (SNR) is set to be 10 dB. Also, all users are i.i.d. and randomly generated.

Fig. 3 demonstrates the OP of FAMA against the number of observed ports for different values of target SINR γ. The label "Reference" in the results indicates the situation which uses the observations only to select the best port, while the label "Ideal" indicates the scenario where the underlying channel of all ports is known and the best port is always selected. Finally, the label "Proposed" indicates the usage of the cGAN-based channel gain generation to find the missing SINRs for selecting the port. As expected in Fig. 3, increasing W reduces the OP because FAS has greater ability to avoid the interference by selecting the optimal port. Additionally, a greater number of observations correlates with lower OP. Furthermore, as anticipated, OP rises with increasing the target SINR, γ.

In Fig. 4, we plot the OP and multiplexing gain against the number of UEs for different values of W with $N = 144$ and $\gamma = 0$ dB. In the simulations, we have assumed that only 20% of the ports are observed. It can be observed that initially the OP is low which leads to the multiplexing gain reaching its upper bound. Also, by increasing the number of users, the multiplexing gain also increases which shows that the FAS at each UE can resolve the inter-user interference. However, by further increasing the number of users, the system reaches its capacity of serving the maximum number of users and the OP then increases, suppressing the multiplexing gain.

Fig. 5 illustrates the OP and multiplexing gain results but against the size of FAS W with $N = 144$ and $\gamma = 0$ dB. As before, it is assumed that only 20% of the ports are observed. The results indicate that as the FAS size increases, the likelihood of finding a port where interference is minimized increases, and thus the multiplexing gain increases by switching to the best port. The proposed cGAN method also successfully generated the envelope of the SINR, even for large W values, resulting in a small performance loss compared with the ideal scenario in which all ports are observed.

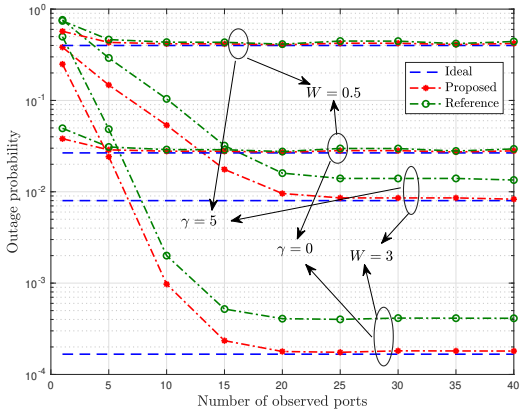

Fig. 3: OP against the number of observed ports with the total number of ports $N = 144$ and $U = 2$.

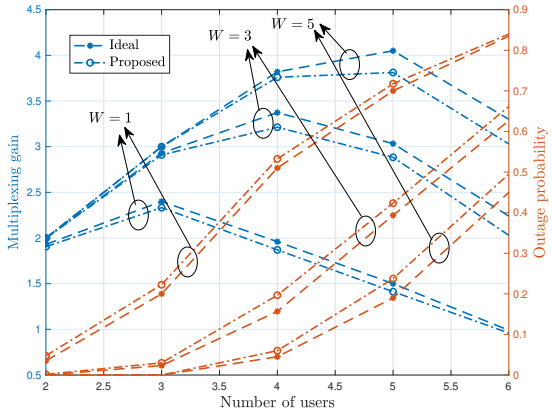

Fig. 4: OP and multiplexing gain against the number of users with the total number of ports $N = 144$ and the SINR target $\gamma = 0$ dB when 20% of the ports are observed.

Finally, Fig. 6 illustrates the OP against the number of ports N. Here, a comparison is made between the proposed cGAN approach with the LSTM approach in [20]. For the both cGAN and LSTM methods, it is assumed that only 25% of the ports are observed. The results demonstrate that when $W = 0.5$, the LSTM method and the proposed cGAN method have the same performance. Additionally, for $W = 0.5$, i.e., the size of FAS is relatively small,[8] there is significant correlation among the ports and as a result, it is easy for either LSTM or cGAN to figure out the trend of the SINR envelope. By

[8]What is considered 'small' varies with the actual operating frequency. In this letter, the results may be interpreted as having an operating frequency of $f = 10$ GHz with the size W representing what is feasible for a laptop-sized FAS and they ensure that the channel exhibits rich scattering.

This article has been accepted for publication in IEEE Wireless Communications Letters. This is the author's version which has not been fully edited and content may change prior to final publication. Citation information: DOI 10.1109/LWC.2024.3452941

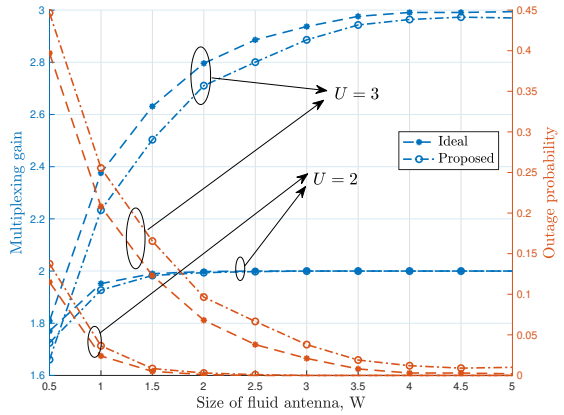

Fig. 5: OP and multiplexing gain against the size of the fluid antenna, W with $N = 144$ and $\gamma = 0$ dB.

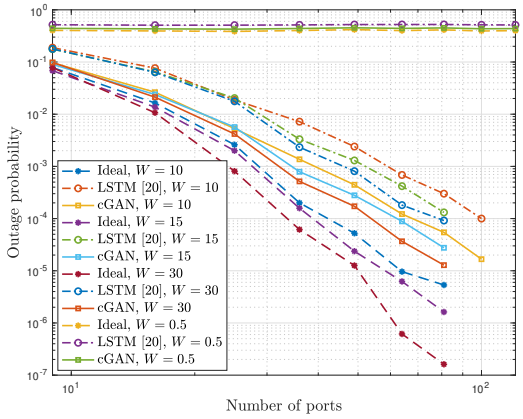

Fig. 6: OP against the number of ports, N with $U = 3$ users in the network and $\gamma = 0$ dB.

increasing W, the cGAN method begins to surpass the LSTM method. This demonstrates the robustness and capability of the proposed cGAN method in estimating the missing port-SINRs when dealing with a large number of ports, confirming the superiority of the proposed approach.

V. Conclusion

In this letter, the port selection problem in slow FAMA systems was addressed, with an emphasis that this was performed with only few SINR observations made. Using the limited SINR observations from the observed ports, we have proposed a cGAN-based solution to generate the SINR envelope for the unobserved ports. Our results have shown that the cGAN can generate accurate results when only a small subset of the ports are available. The results also revealed that the proposed cGAN solution can greatly reduce the OP even when less than 20% of the ports were observed.

References

[1] P. von Butovitsch *et al.*, "Advanced Antenna Systems for 5G Networks," 2019. [Online]. Available: https://www.ericsson.com/en/whitepapers/advanced-antenna-systems-for-5g-networks

[2] K. K. Wong, K. F. Tong, Y. Shen, Y. Chen, and Y. Zhang, "Bruce Lee-inspired fluid antenna system: Six research topics and the potentials for 6G," *Frontiers Commun. and Netw., section Wireless Commun.*, vol. 3, no. 853416, Mar. 2022.

[3] K.-K. Wong, W. K. New, X. Hao, K.-F. Tong, and C.-B. Chae, "Fluid antenna system—part I: Preliminaries," *IEEE Commun. Lett.*, vol. 27, no. 8, pp. 1919–1923, Aug. 2023.

[4] K. K. Wong, A. Shojaeifard, K. F. Tong, and Y. Zhang, "Performance limits of fluid antenna systems," *IEEE Commun. Lett.*, vol. 24, no. 11, pp. 2469–2472, Nov. 2020.

[5] K.-K. Wong, A. Shojaeifard, K.-F. Tong, and Y. Zhang, "Fluid antenna systems," *IEEE Trans. Wireless Commun.*, vol. 20, no. 3, pp. 1950–1962, Mar. 2021.

[6] M. Khammassi, A. Kammoun and M.-S. Alouini, "A new analytical approximation of the fluid antenna system channel," *IEEE Trans. Wireless Commun.*, vol. 22, no. 12, pp. 8843–8858, Dec. 2023.

[7] J. D. Vega-Sánchez, A. E. López-Ramírez, L. Urquiza-Aguiar and D. P. M. Osorio, "Novel expressions for the OP and diversity gains in fluid antenna system," *IEEE Wireless Commun. Lett.*, vol. 13, no. 2, pp. 372–376, Feb. 2024.

[8] J. D. Vega-Sánchez, L. Urquiza-Aguiar, M. C. P. Paredes and D. P. M. Osorio, "A simple method for the performance analysis of fluid antenna systems under correlated Nakagami-m fading," *IEEE Wireless Commun. Lett.*, vol. 13, no. 2, pp. 377–381, Feb. 2024.

[9] P. D. Alvim *et al.*, "On the performance of fluid antennas systems under α-μ fading channels," *IEEE Wireless Commun. Lett.*, vol. 13, no. 1, pp. 108–112, Jan. 2024.

[10] C. Psomas, P. J. Smith, H. A. Suraweera and I. Krikidis, "Continuous fluid antenna systems: Modeling and analysis," *IEEE Commun. Lett.*, vol. 27, no. 12, pp. 3370–3374, Dec. 2023.

[11] W. K. New, K. K. Wong, H. Xu, K. F. Tong and C.-B. Chae, "An information-theoretic characterization of MIMO-FAS: Optimization, diversity-multiplexing tradeoff and q-outage capacity," *IEEE Trans. Wireless Commun.*, vol. 23, no. 6, pp. 5541–5556, Jun. 2024.

[12] L. Zhu, and K. K. Wong, "Historical review of fluid antennas and movable antennas," *arXiv preprint*, arXiv:2401.02362v2, Jan. 2024.

[13] Y. Shen *et al.*, "Design and implementation of mmWave surface wave enabled fluid antennas and experimental results for fluid antenna multiple access," *arXiv preprint*, arXiv:2405.09663, May 2024.

[14] J. Zhang *et al.*, "A pixel-based reconfigurable antenna design for fluid antenna systems," *arXiv preprint*, arXiv:2406.05499, Jun. 2024.

[15] K. K. Wong and K. F. Tong, "Fluid antenna multiple access," *IEEE Trans. Wireless Commun.*, vol. 21, no. 7, pp. 4801–4815, Jul. 2022.

[16] K. K. Wong, K. F. Tong, Y. Chen, and Y. Zhang, "Fast fluid antenna multiple access enabling massive connectivity," *IEEE Commun. Lett.*, vol. 27, no. 2, pp. 711–715, Feb. 2023.

[17] K. K. Wong, D. Morales-Jimenez, K. F. Tong, and C. B. Chae, "Slow fluid antenna multiple access," *IEEE Trans. Commun.*, vol. 71, no. 5, pp. 2831–2846, May 2023.

[18] Z. Chai, K.-K. Wong, K.-F. Tong, Y. Chen, and Y. Zhang, "Port selection for fluid antenna systems," *IEEE Commun. Lett.*, vol. 26, no. 5, pp. 1180–1184, May 2022.

[19] J. Zou, S. Sun and C. Wang, "Online learning-induced port selection for fluid antenna in dynamic channel environment," *IEEE Wireless Commun. Lett.*, vol. 13, no. 2, pp. 313–317, Feb. 2024.

[20] N. Waqar, K.-K. Wong, K.-F. Tong, A. Sharples, and Y. Zhang, "Deep learning enabled slow fluid antenna multiple access," *IEEE Commun. Lett.*, vol. 27, no. 3, pp. 861–865, Mar. 2023.

[21] M. Mirza and S. Osindero, "Conditional generative adversarial nets," *arXiv preprint*, arXiv:1411.1784, 2014.

[22] G. L. Stüber and G. L. Steuber, *Principles of mobile communication*, 2nd ed. Springer, 2001.

[23] K.-K. Wong, K.-F. Tong, Y. Chen, and Y. Zhang, "Closed-form expressions for spatial correlation parameters for performance analysis of fluid antenna systems," *Electron. Lett.*, vol. 58, no. 11, pp. 454–457, Apr. 2022.

[24] P. Isola, J.-Y. Zhu, T. Zhou, and A. A. Efros, "Image-to-image translation with conditional adversarial networks," in *Proc. IEEE Conf. Comput. Vision & Pattern Recog.*, pp. 1125–1134, 21-26 Jul. 2017, Honolulu, HI, USA.

[25] Y. Dong, H. Wang, and Y.-D. Yao, "Channel estimation for one-bit multiuser massive MIMO using conditional GAN," *IEEE Commun. Lett.*, vol. 25, no. 3, pp. 854–858, Mar. 2021.